RESEARCH ARTICLE

Figures and figure supplements

EHD2 overexpression promotes tumorigenesis and metastasis in triple-negative breast cancer by regulating store-operated calcium entry

Haitao Luan, Timothy A Bielecki and Bhopal C Mohapatra *et al*.

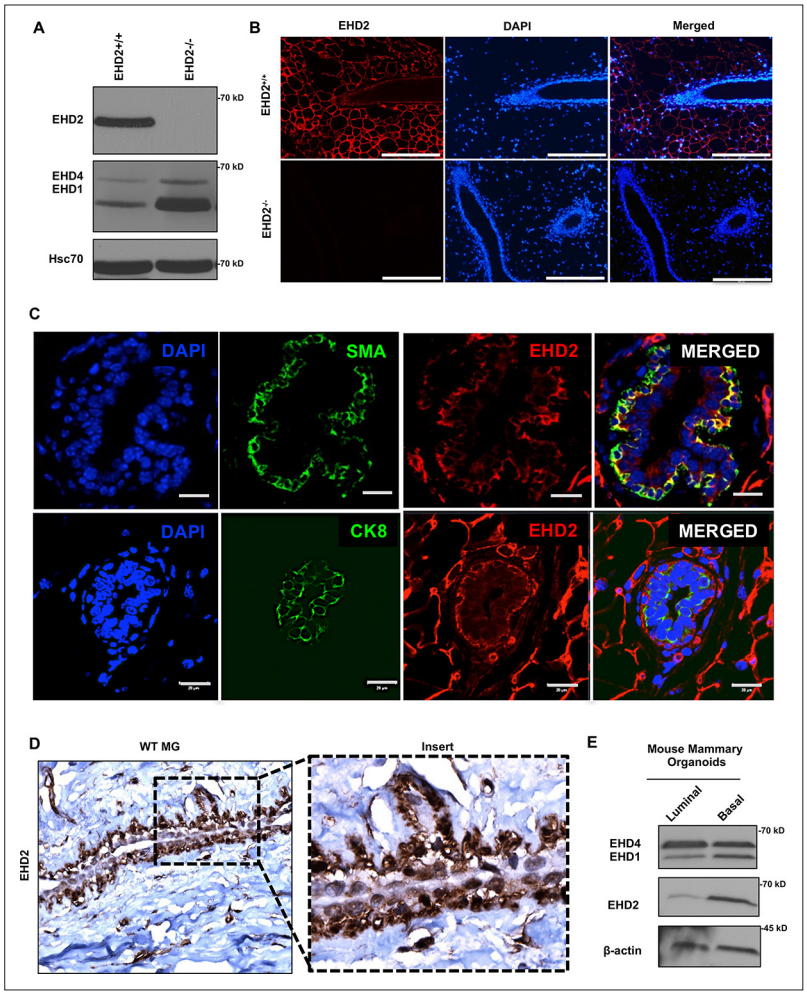

Figure 1. EHD2 is expressed in basal-like mammary epithelial cells. (**A and B**) Immunoblot (A) and immunofluorescence (B; scale bar, 20 μm) analysis of wildtype (*Ehd2*+/+) and *Ehd2*-null (*Ehd2*-/-) mouse mammary gland to validate the specific reactivity of anti-EHD2 antibody used in this study. (**C**) Immunofluorescence analysis of EHD2 expression in basal vs. luminal epithelial cells of normal mouse mammary gland. Top panel, EHD2 (red) co-staining with basal cell marker alpha smooth muscle actin (SMA; green); Bottom panel, EHD2 (red) co-staining with luminal cell marker cytokeratin 8 (CK8; green). Nuclei are stained with DAPI (blue). Scale bars, 20 μm. (**D**) Confirmation of the basal epithelial cell-selective EHD2 expression in mouse mammary gland by immunohistochemical staining. Magnification, 200X. (**E**) Predominant basal epithelial cell expression of EHD2 revealed by immunoblot analysis of Matrigel-grown organoids derived from FACS-sorted EPCAM-low/CD29-high (basal) vs. EPCAM-high/CD29-low (luminal) mouse mammary epithelial cell populations.

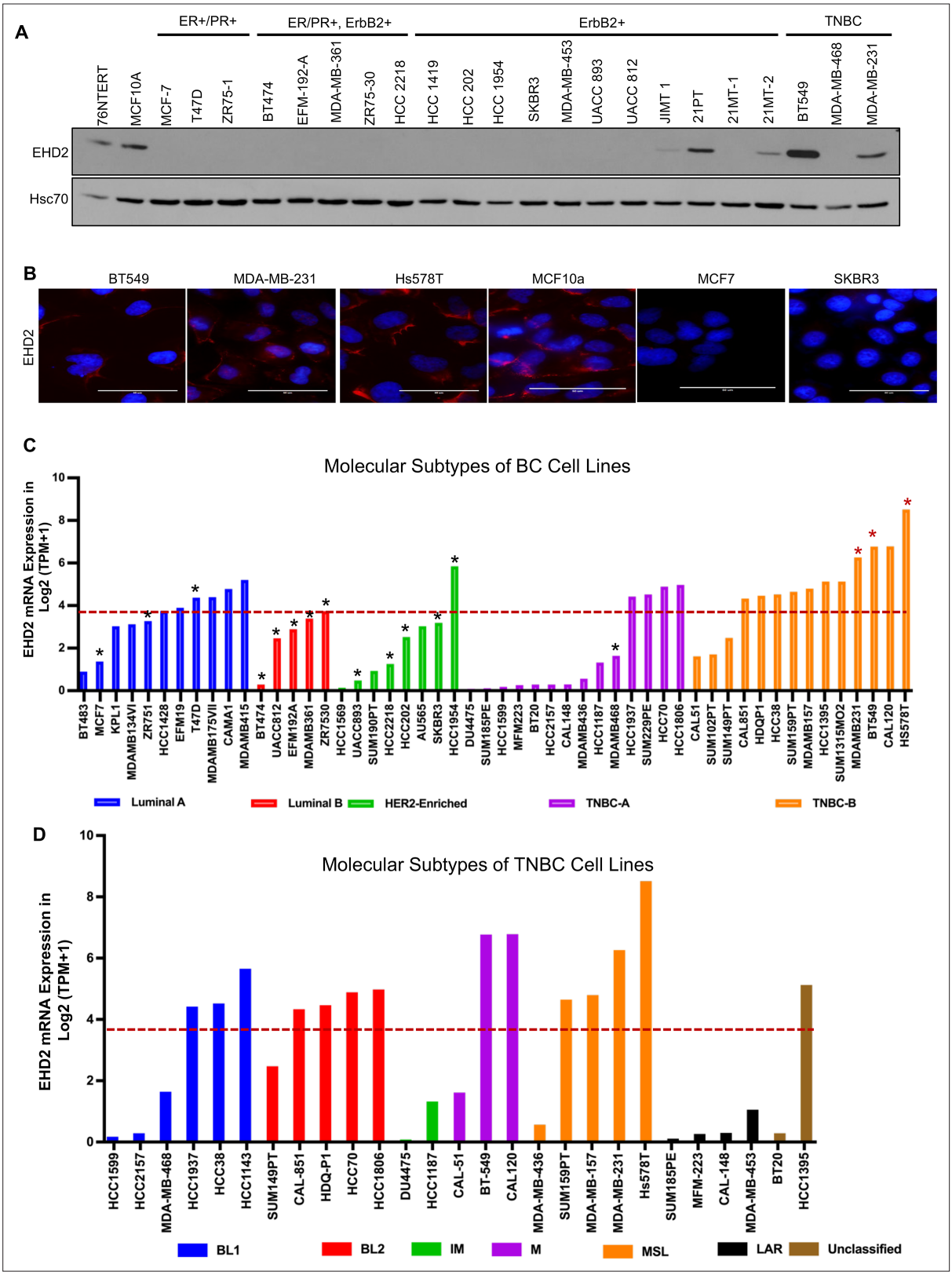

Figure 2. High EHD2 expression is preferentially observed in basal-like immortal mammary epithelial cell lines and in triple-negtaive/basal and HER2+ breast cancer cell lines. (**A**) Immunoblot analysis of EHD2 expression in non-tumorigenic immortal basal-like (76Ntert, MCF10a), and luminal A (ER+/PR+), luminal B (ER+/PR+, ErbB2+), ErbB2+, and Triple-negative (TN) breast cancer cell lines. (**B**) Immunofluorescence microscopy analysis of selected cell lines from A to further validate EHD2 (Red) expression pattern, showing predominant cytoplasmic and membrane localization. DAPI (blue) marks the

Figure 2 continued on next page

Figure 2 continued

nuclei. Scale bar, 50 μm. (**C**) EHD2 mRNA expression in breast cancer cell lines corresponding to major molecular subtypes as described in ***Dai et al., 2017***. (**D**) EHD2 mRNA expression in breast cancer cell lines corresponding to TNBC subtypes as described in ***Lehmann et al., 2011***. In C and D, The CCLE mRNA expression data is obtained as follows (per the CCLE site): RNASeq files are aligned with STAR and quantified with RSEM, and then TPM normalized. Reported values are Log2 (TPM + 1); TPM, transcripts per million. The dotted line represents the median expression value of EHD2 among all (N=63) BC cell lines. The black and red asterisks (*) in C indicate cell lines that we show as negative or positive for EHD2 expression by western blotting or immunofluorescence microscopy (**A** and **B**).

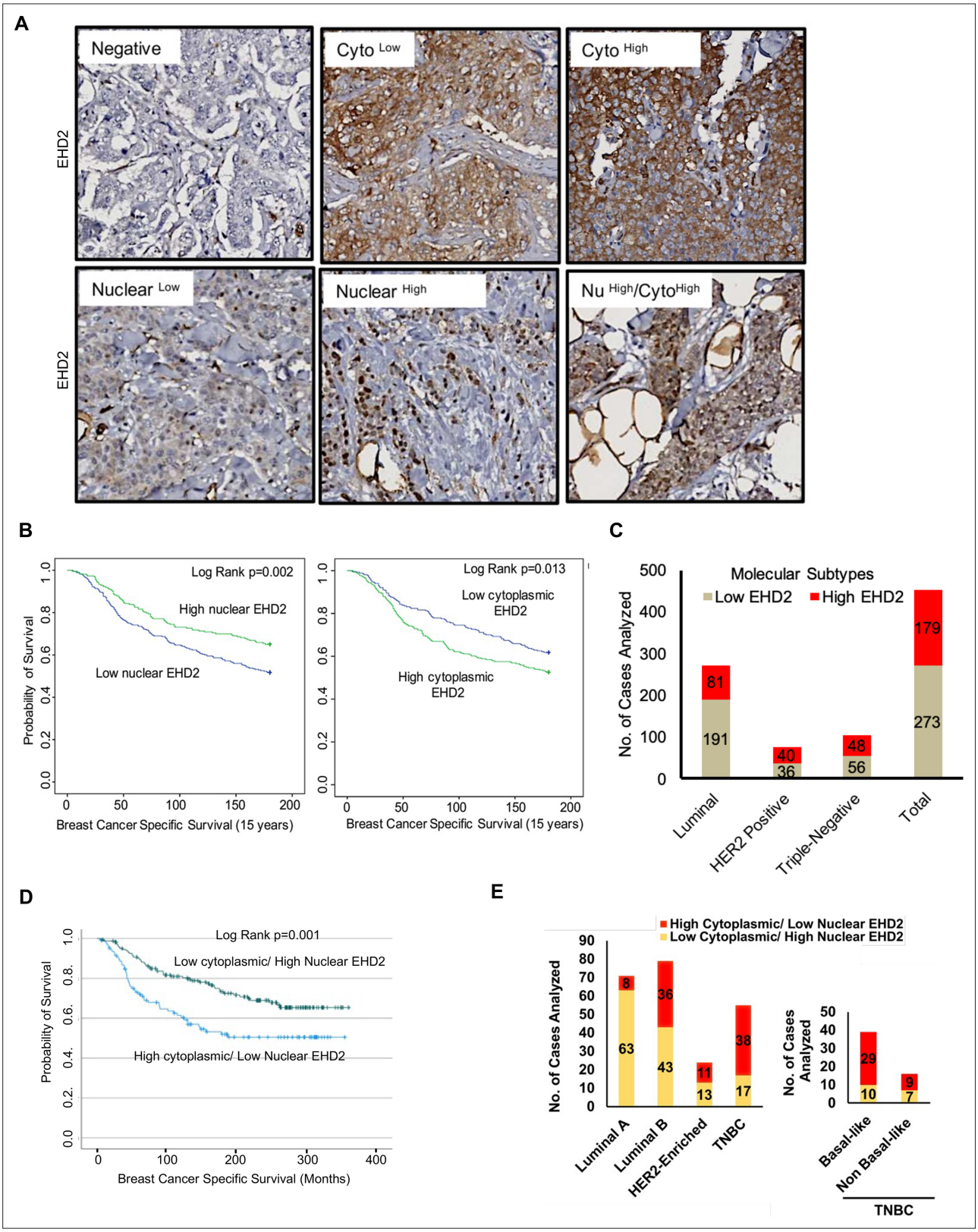

Figure 3. EHD2 is overexpressed in a subset of breast cancer patients and is associated with metastasis and shorter survival. (**A**) Representative images of negative/low/high cytoplasmic and nuclear EHD2 IHC staining of a breast cancer tumor microarray (840 samples). Magnification, 20X. (**B**) Kaplan-Meier survival curves correlating positive/high (green) vs. low/negative (blue) nuclear (left panel; N=288 vs 458) or cytoplasmic (right panel; N=392 vs 352) EHD2 expression with Breast Cancer Specific Survival (BCSS). (**C**) Number (Y-axis) of cytoplasmic EHD2-negative/low (gray) and -positive/

Figure 3 continued on next page

Figure 3 continued

high samples among ER/PR+, ErbB2+, TN, and all tumors. (**D**) Kaplan-Meier survival analysis of a subset of patients with molecular subtyping markers available (N=271) comparing high cytoplasmic/low nuclear (blue; N=107 out of 271) vs low cytoplasmic/high nuclear (green; N=164 out of 271). (**E**) Left panel - number (Y-axis) of high cytoplasmic/low nuclear EHD2 (red) and low cytoplasmic /high nuclear EHD2 (yellow) cases (among the 271 cases analyzed in D) within the luminal A (ER^+/PR^+, $HER2^-$ and Ki67 <14%), luminal B (ER^+/PR^+ or $^-$ and either $HER2^+$ or Ki67 >/=14% or both), HER2-Enriched (ER^-, PR^- and $HER2^+$, regardless of the Ki67) and TNBC (ER, PR and $HER2^-$, regardless of the Ki67) BC subtypes. Right panel - number of high cytoplasmic/low nuclear (red) or low cytoplasmic/high nuclear (yellow) EHD2 staining in basal-like (CK5/6 or CK14 or CK17 positive) and non-basal-like (CK5/6, CK14 or CK17 negative) TNBC subtypes.

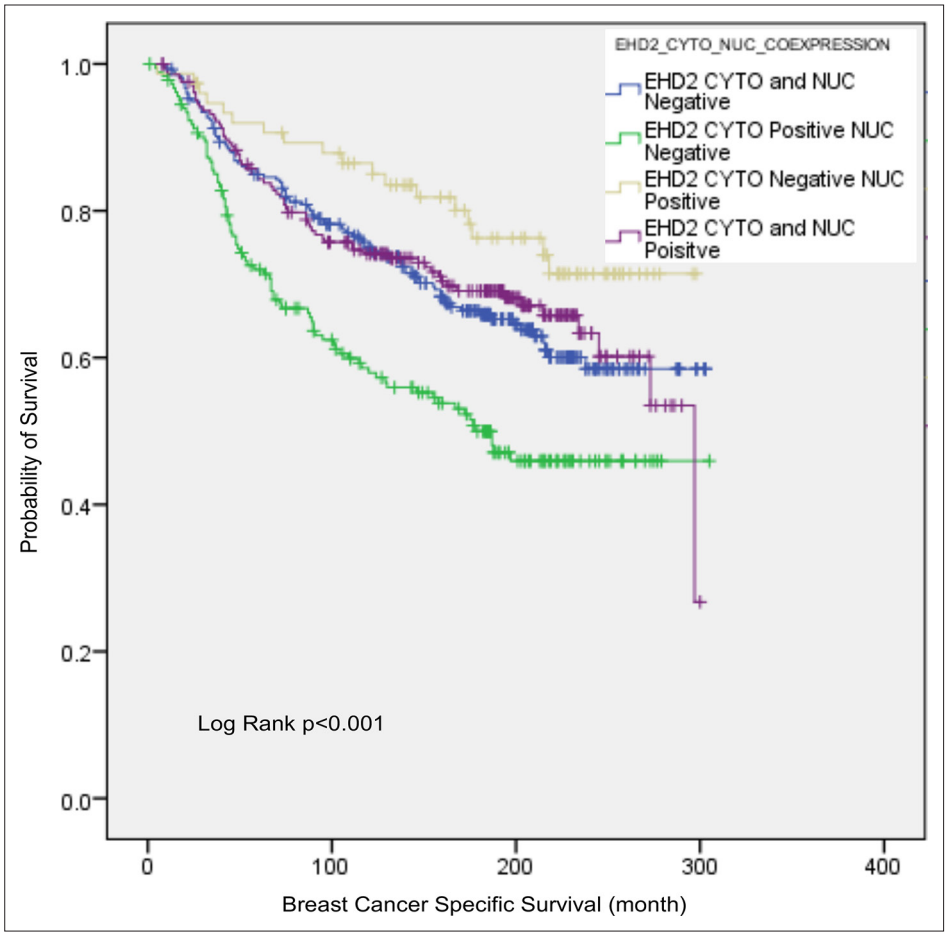

Figure 3—figure supplement 1. Kaplan-Meier survival curve for Breast Cancer Specific Survival (BCSS) probability in all tumors scored for cytoplasmic and nuclear positive (purple), cytoplasmic and nuclear negative (blue), cytoplasmic positive and nuclear negative (green), cytoplasmic negative and nuclear positive (yellow) EHD2 expression. N=275 for cytoplasmic and nuclear negative, 183 for cytoplasmic positive and nuclear negative, 76 for cytoplasmic negative and nuclear positive and 207 for cytoplasmic and nuclear positive.

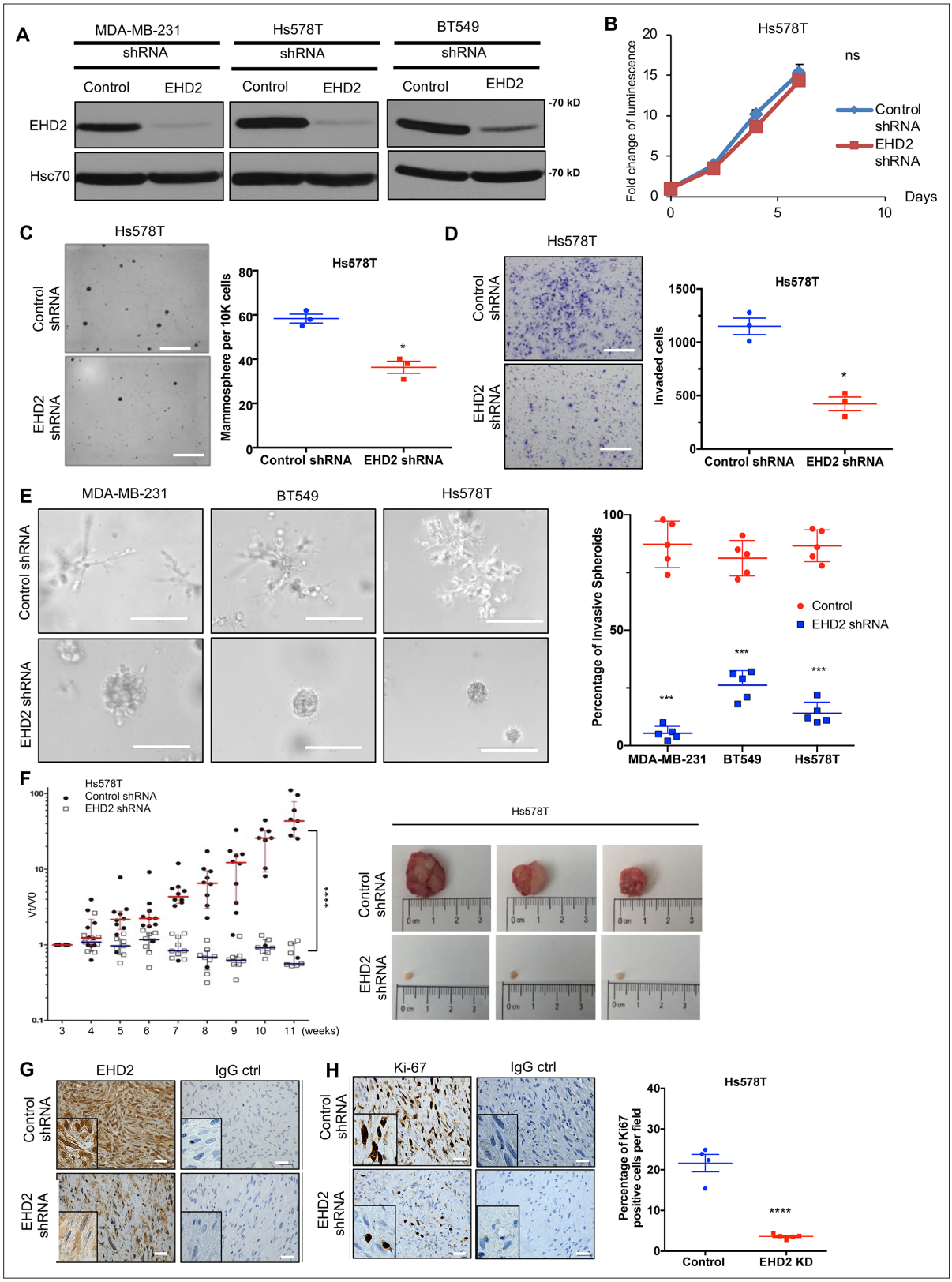

Figure 4. *EHD2* knockdown in TNBC cell lines impairs the tumorigenic and pro-metastatic traits. (**A**) Immunoblot confirmation of shRNA-mediated *EHD2* knockdown. (**B**) Cell Titer-Glo proliferation (2000 cells/well; 24 replicates each) over time. Mean +/- SEM, n=3, ns, not significant. (**C**) Tumorsphere formation quantified on day 7. Left, representative images; Right, quantification of tumorspheres/well. Mean +/- SEM, n=3, *p<0.05; **p<0.01. Scale bar, 400 µm. (**D**) Transwell invasion of cells plated in 0.5% FBS medium towards complete medium assayed after 18 hr. Left, representative images; Right,

Figure 4 continued on next page

Figure 4 continued

quantification of invaded cells (Mean +/- SEM, n=3, *p<0.05). Scale bar, 400 μm. (**E**) Three-dimensional invasion in Matrigel-grown organoids. A total of 2000 cells plated per well in 50% Matrigel on top of 100% Matrigel layer in eight-well chamber slides for 7 days before imaging. Left, representative images; right, % spheroids with invasive fronts from over 100 counted per well, n=4, *** p<0.001. Scale bar, 200 μm. (**F**) Xenograft tumorigenesis. Four-week-old nude mice orthotopically-injected with $5x10^6$ cells were followed over time. Left, fold change in tumor volume over time for individual mice. Mean (red/blue lines) +/- SEM; ****p<0.0001 by two-way ANOVA. Right, representative tumors (close to median of groups). (**G, H**) Representative IHC staining of tumor sections for EHD2 (**G**) or Ki67 (**H**), with respective controls. Right, Mean +/- SEM of Ki67 + staining. ****, p<0.0001. Scale bar, 25 μm.

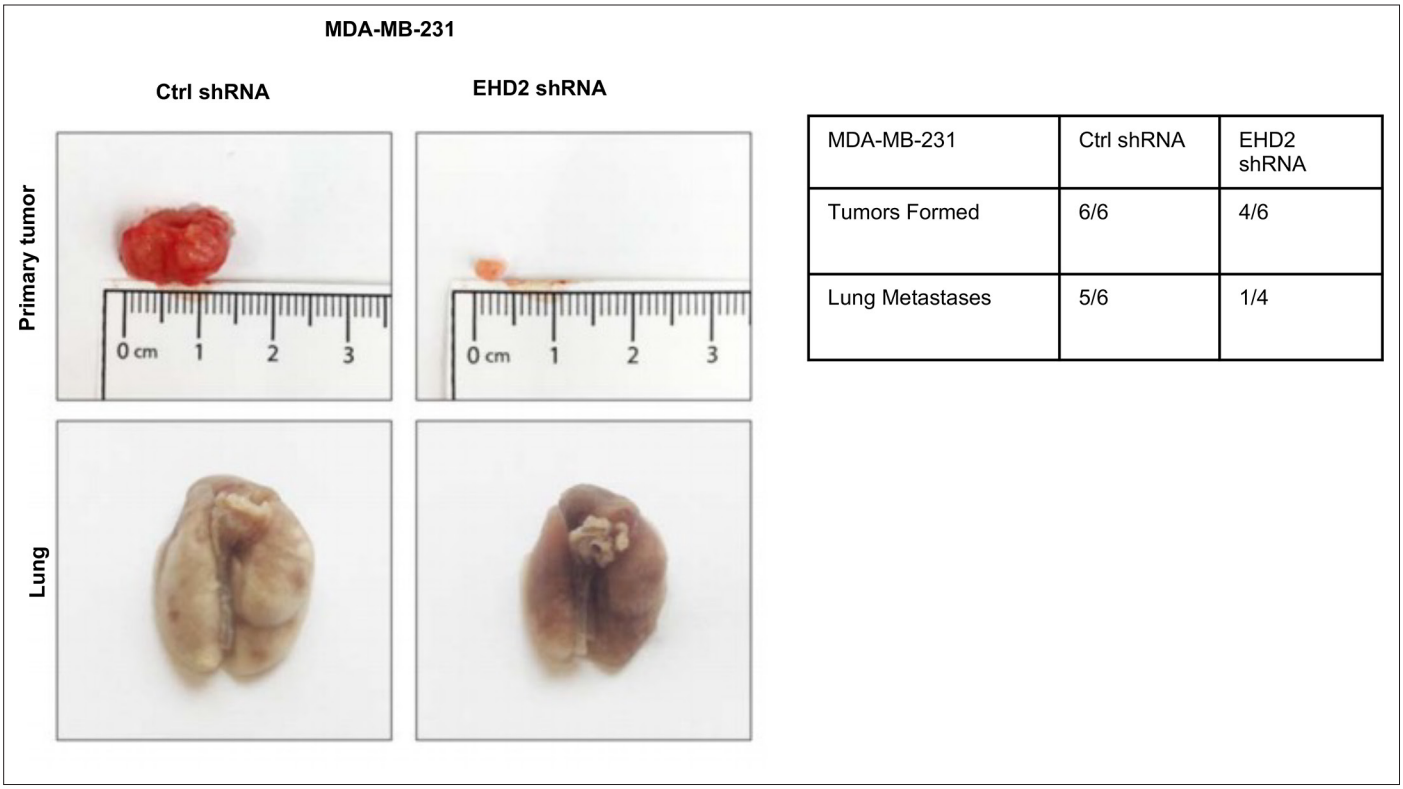

MDA-MB-231	Ctrl shRNA	EHD2 shRNA
Tumors Formed	6/6	4/6
Lung Metastases	5/6	1/4

Figure 4—figure supplement 1. Knockdown of *EHD2* impaired the tumorigeneses and metastases in vivo. Primary tumor xenograft tumorigenesis and lung metastasis of MDA-MB-231 cells expressing control or *EHD2* shRNA. Representative primary tumors and lungs are shown on left. Table on right shows the numbers of mice developing identifiable primary tumors and lung metastases.

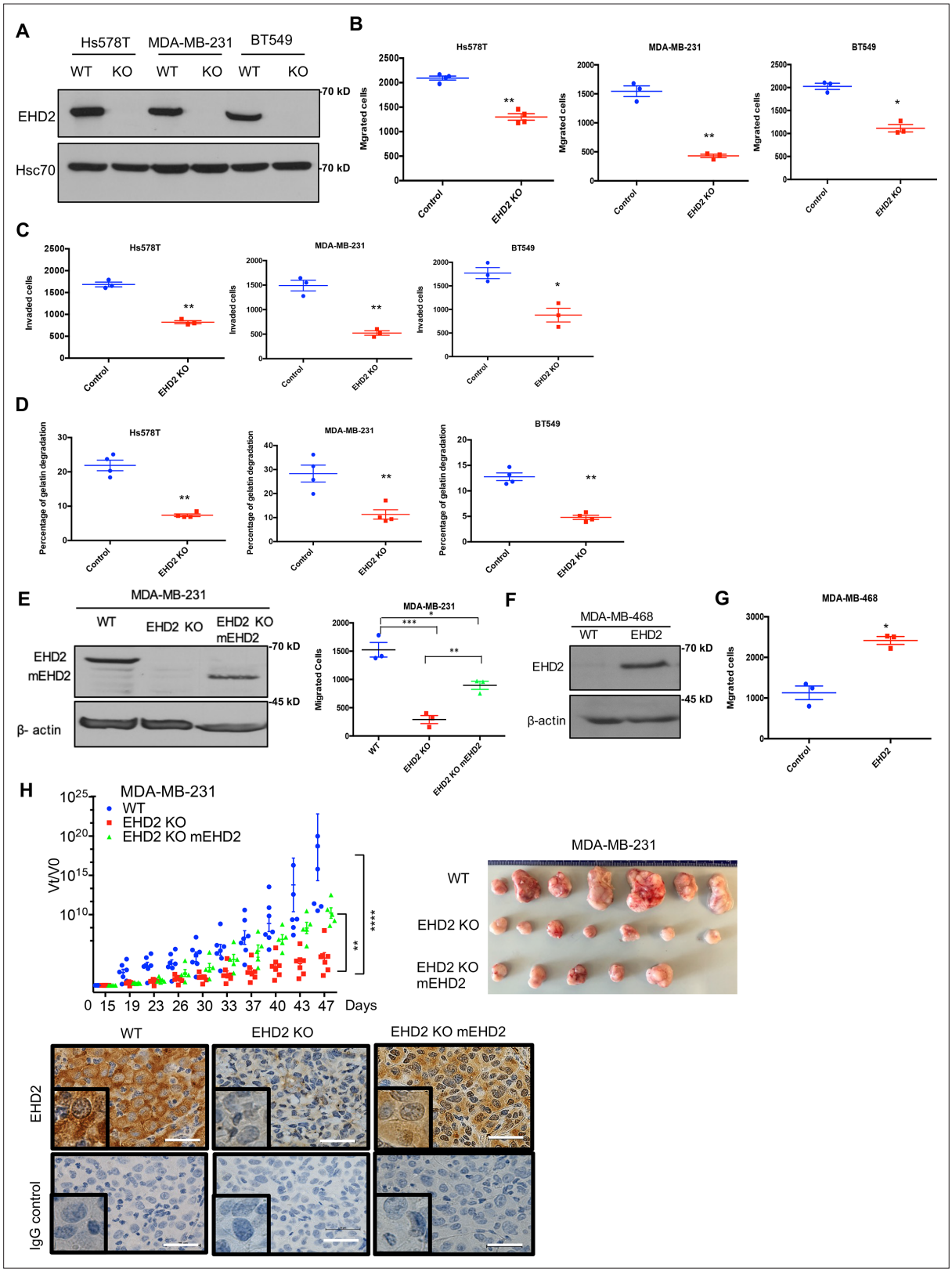

Figure 5. *EHD2* knockout in TNBC cell lines impairs the tumorigenic and pro-metastatic traits. Single cell clones of TNBC cell lines serially transduced with Cas9 and control or *EHD2* sgRNA lentiviruses were obtained and used as a pool of >3 clones. (**A**) Immunoblotting of EHD2 expression in KO vs. WT (Cas9) controls. (**B**) Transwell migration. Data points are independent experiments; Mean +/- SEM of migrated cells (input 10 K), **p<0.01, *p<0.05. (**C**) Transwell invasion across Matrigel. Mean +/- SEM of invaded cells (input 10 K), **p<0.01, *p<0.05. (**D**) Extracellular matrix degradation. Cells plated

Figure 5 continued on next page

Figure 5 continued

on Cy5-gelatin and percentage area with matrix degradation quantified after 48 hr. Mean +/- SEM, **p<0.01. (**E**) Mouse *Ehd2* rescue of *EHD2*- KO MDA-MB-231 cells. Left, immunoblot to show re-expression of mouse EHD2; beta-actin, loading control. Right, rescue of cell migration defect. Mean +/- SEM, ***p<0.001, **p<0.01, *p<0.05. (**F–G**) CRISPRa induction of endogenous *EHD2* expression in EHD2-negative MDA-MB-468 cell line (**F**) and increase in migration (**G**). Mean +/- SEM, *p<0.05. (**H**) Impairment of tumorigenesis by *EHD2*-KO and rescue by mouse *Ehd2* reconstitution. Left, groups of eight nude mice orthotopically implanted with $3x10^6$ cells and tumors analyzed as in ***Figure 4F***: ****p<0.0001, **p=0.001. Right, Representative tumor images. Bottom, representative tumor sections stained for EHD2 and control. Scale bar, 25 μm.

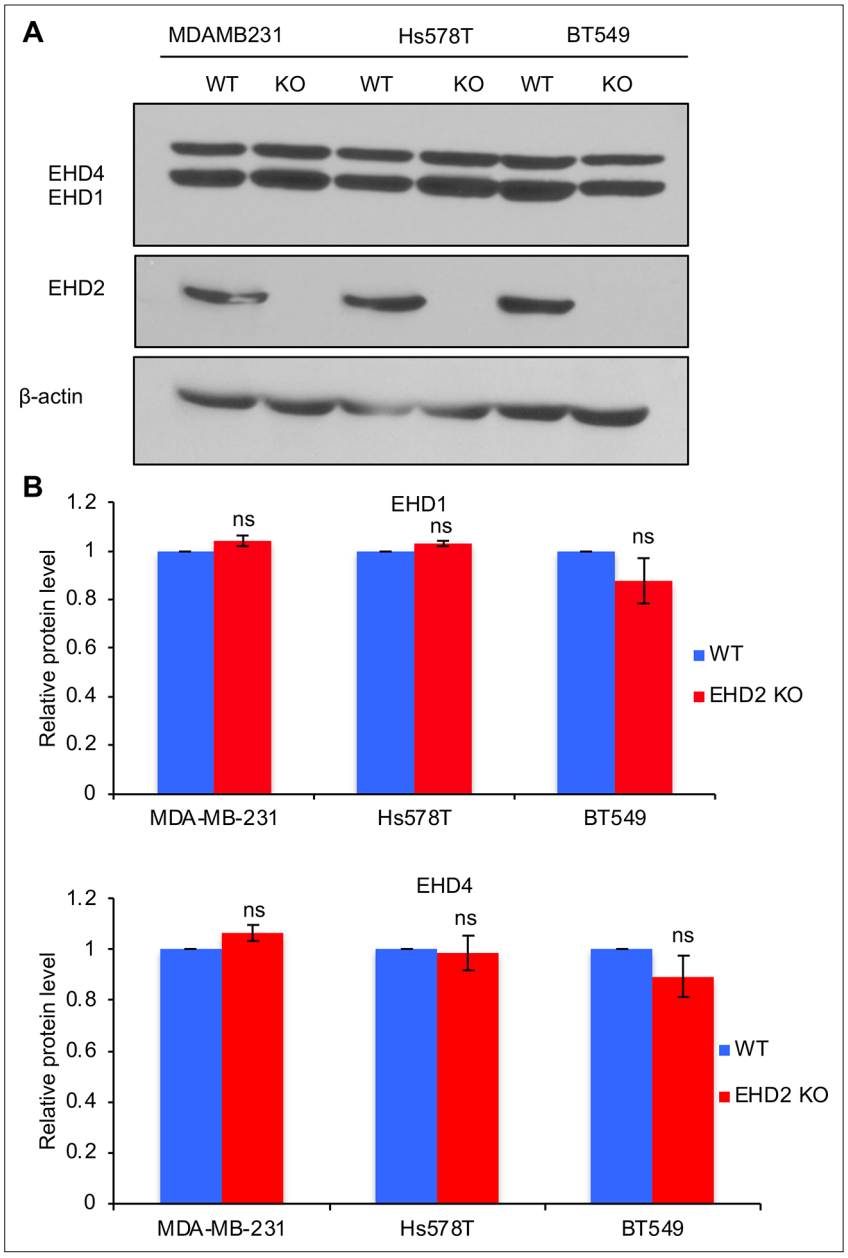

Figure 5—figure supplement 1. EHD1/4 expression is unchanged in *EHD2* knockout TNBC cell lines. (**A**) Immunoblot analysis of EHD1/4 expression in *EHD2* WT and KO MDA-MB-231, Hs578t and BT549 breast cancer cell lines. (**B**) Densitometric quantification of EHD1/4 expression levels from three independent experiments; ns, not significant (Student's t test).

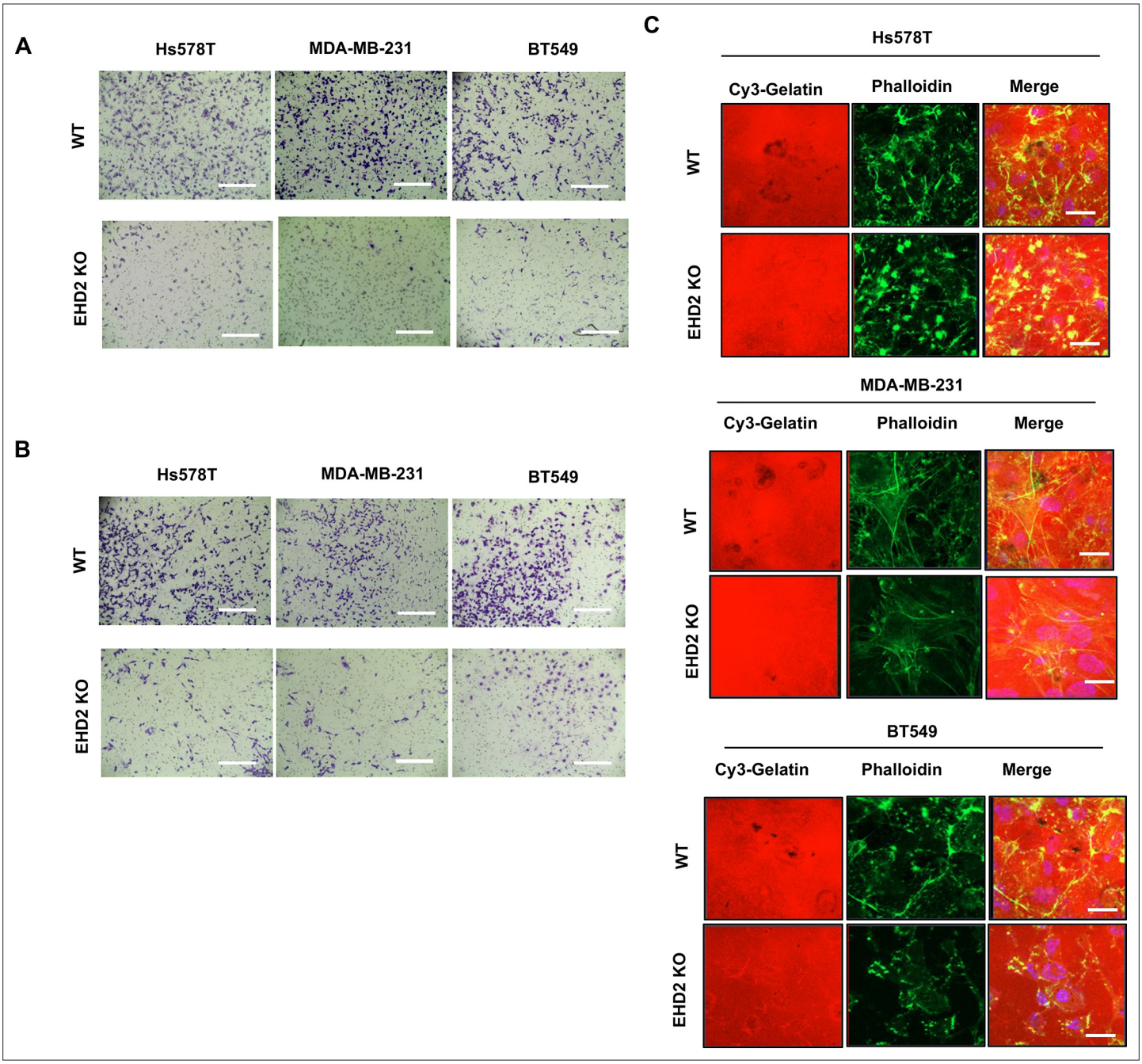

Figure 5—figure supplement 2. Loss of EHD2 decreased oncogenesis traits in TNBC cells. (**A**) Representative images of cell migration in control and *EHD2*-KO TNBC cells. Scale bar, 400 μm. (**B**) Representative images of cell invasion in control and *EHD2*-KO TNBC cells. Scale bar, 400 μm. (**C**) Representative images of extracellular matrix degradation in control and *EHD2*-KO TNBC cells. Scale bar, 10 μm.

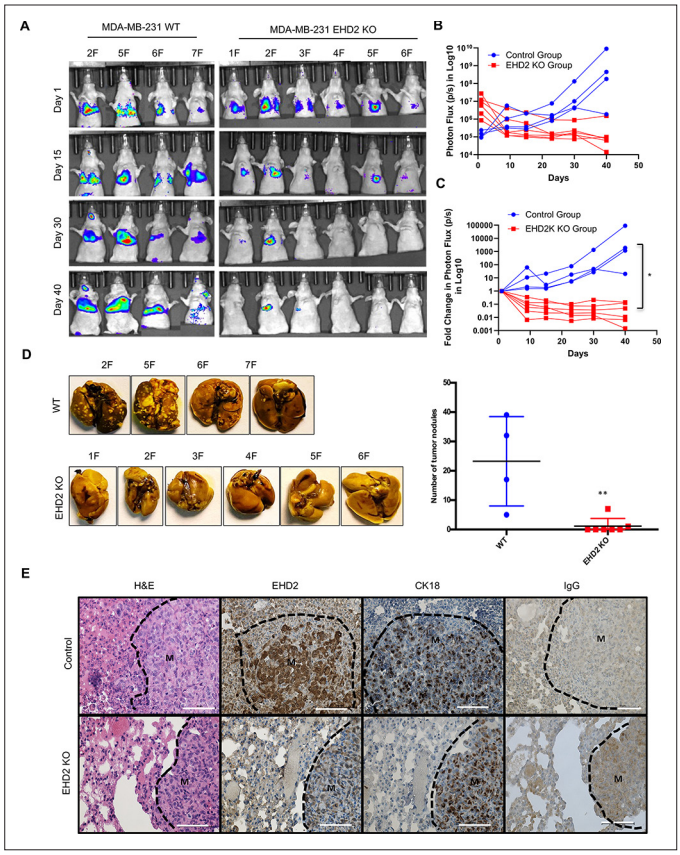

Figure 6. *EHD2* KO impairs the ability of TNBC cells to form lung metastases. WT control and *EHD2*-KO MDA-MB-231 cells were engineered with tdTomato-luciferase and 10^6 cells of each injected intravenously into groups of seven nude mice. Lung metastases were monitored by bioluminescence imaging (**A**) Bioluminescence images of mice over time. . (**B–C**) Bioluminescence signals over time (Control, blue; KO, red) are shown as either untransformed photon flux values (**B**) or log fold-change in photon flux relative to day 0 (**C**). Two-way ANOVA showed the differences between Control and KO groups to be significant (*p<0.05). (**D**) Left panel, images of lungs harvested at necropsy show nearly complete absence of metastatic nodules in lungs of mice injected with *EHD2*-KO cells. Right panel, quantification of tumor nodules in the lungs, **, p<0.01. (**E**) Representative H&E (first panels), EHD2 (second panels), CK18 (third panels) and control IgG staining (fourth panels) of metastatic lung tissue sections from control (upper) and *EHD2*-KO cell injected mice. Note the retention of normal lung tissue in *EHD2*-KO cell injected mouse lung, and absence of EHD2 expression in KO nodules (labeled M). CK18 demarcates the human tumor cell area. Scale bar, 50 μm.

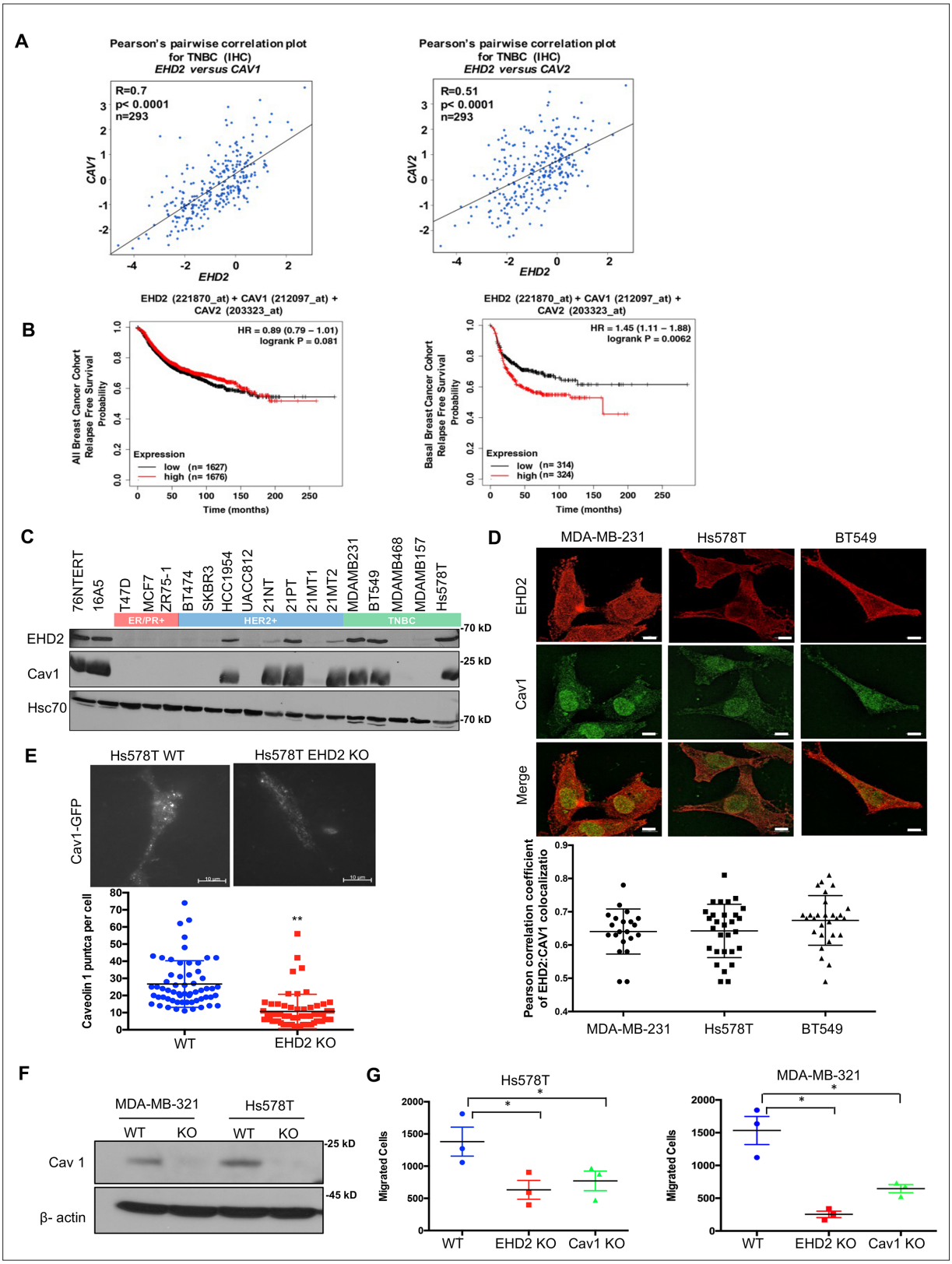

Figure 7. EHD2 and Caveolin-1/2 are co-overexpressed in breast cancers and EHD2 regulates cell surface caveolae. (**A**) Pearson's correlation plots of EHD2/CAV1 and EHD2/CAV2 expression in TNBC (IHC-based) subsets of TCGA and SCAN-B RNAseq datasets analyzed on bc-GenExMiner v4.5 platform. Indicated: n, number of samples; R, correlation coefficients; significance. (**B**) KM plotter analysis of EHD2, CAV1 and CAV2 overexpression correlation with relapse-free survival (RFS) for upper vs. lower quartiles in basal-like breast cancer (PAM50-based) cohorts of TCGA, GEO, and GEA

Figure 7 continued on next page

Figure 7 continued

datasets. Probe sets used: *EHD2* (221870_at), *CAV1* (212097_at) and *CAV2* (203323_at). Analysis of all samples combined found no survival differences (left panel). (**C**) Immunoblot analysis of coordinate EHD2 and CAV1 expression in immortal mammary epithelial cells and breast cancer cell lines. (**D**) SIM images demonstrated colocalization of EHD2 (red) and caveolin-1 (green) in TNBC cell lines; scale bar, 10 μm. Top, representative SIM images; Bottom, Pearson's Coefficient of Colocalization between EHD2 and CAV1 in TNBC cells from three independent experiments. (**E**) TIRF analysis of fluorescent CAV1 puncta to quantify cell surface caveolae pool. Top, representative TIRF images. Bottom, quantification of CAV1 puncta. Mean +/- SEM of puncta per cell pooled from 3 independent experiments; **p<0.01. Scale bar, 10μm. (**F**) Immunoblot confirmation of CRISPR-Cas9 *CAV1*-KO in TNBC cell lines. (**G**) Impact of *CAV1*-KO on Transwell migration. Mean +/- SEM number of migrated cells (input 10 K) per Transwell (n=3, *p<0.05).

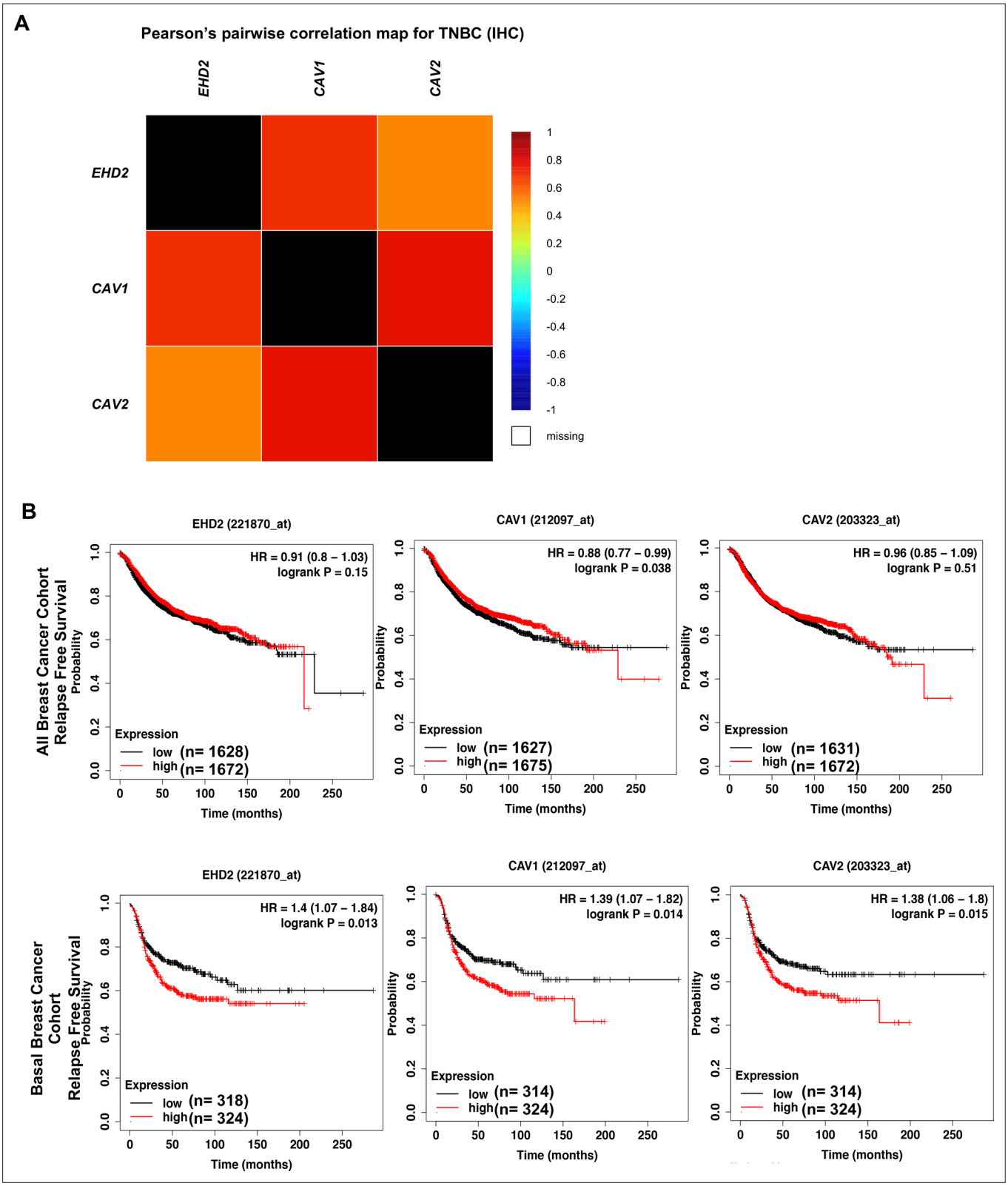

Figure 7—figure supplement 1. EHD2 and Caveolin-1/2 are correlated in breast cancers patients. (**A**) Pearson's pairwise correlation heatmap analysis of the expression of targeted genes (*EHD2, CAV1* and *CAV2*) for the TNBC cohort based on IHC. Analysis used TCGA and SCAN-B RNAseq dataset of bc-GenExMiner v4.5 platform. (**B**) KM plotter analysis of upper vs. lower quartile survival curves display poor relapse-free survival (RFS) associated with EHD2, CAV1, and CAV2 overexpression in basal-like breast cancer (based on PAM50 subtype) cohorts of TCGA, GEO, and GEA datasets (KM plotter).

Figure 7—figure supplement 1 continued on next page

Figure 7—figure supplement 1 continued

The probe sets used were: *EHD2* (221870_at), *CAV1* (212097_at) and *CAV2* (203323_at). Similar analysis on all breast cancer samples in the cohort found no survival differences (lower panel).

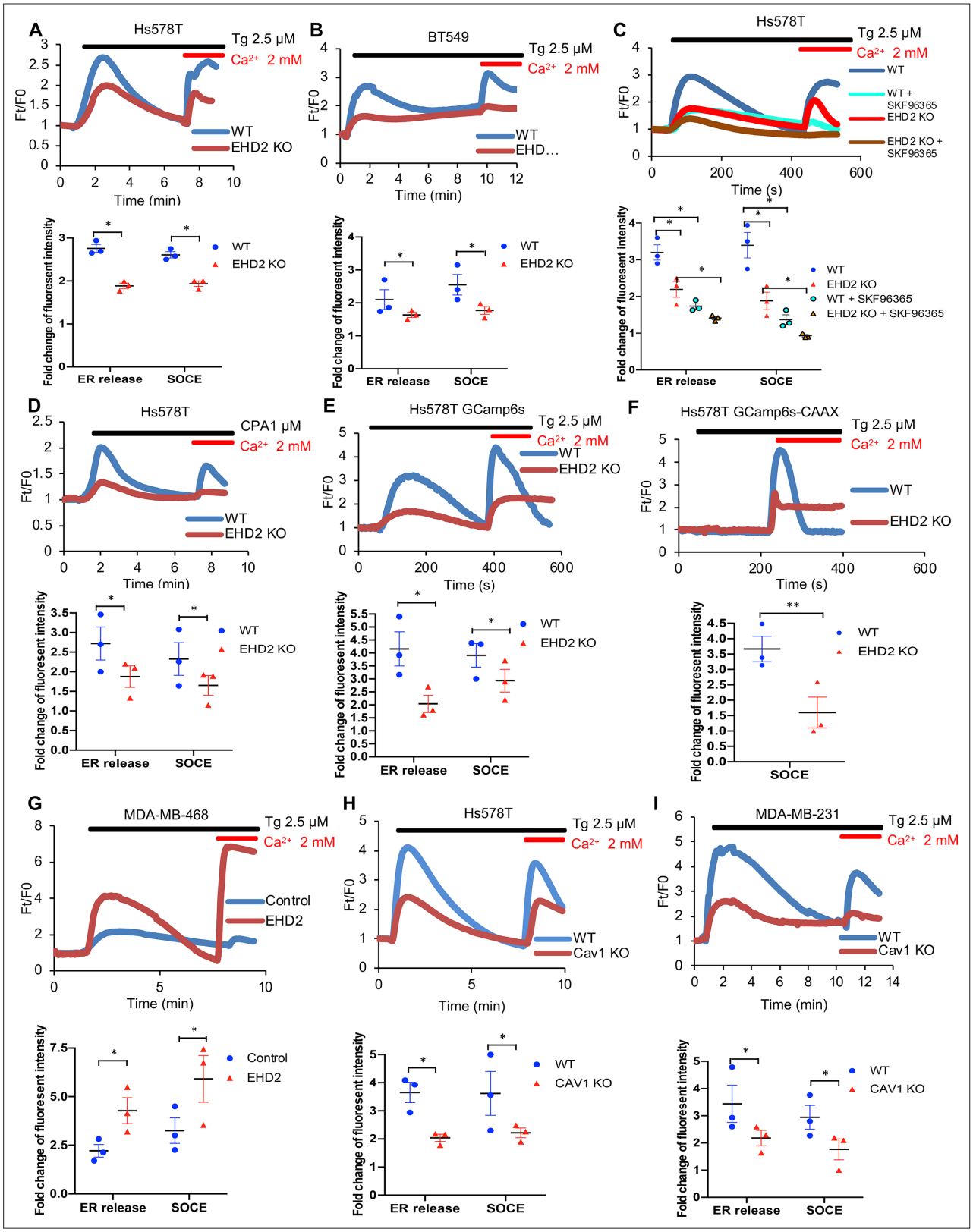

Figure 8. EHD2 promotes store-operated calcium entry (SOCE) in TNBC cell lines. (**A–B**) Thapsigargin (Tg; 2.5 µM)-induced increase in cytoplasmic Ca^{2+} (initial rise in no extracellular Ca^{2+}) and SOCE (second peak after adding 2 mM Ca^{2+}) in Fluo 4 AM-loaded WT/KO Hs578T (**A**) or BT549 (**B**) cell lines measured by live-cell confocal microscopy. (**C**) Impact of SOCE inhibitor SKF96365 (10 µM) on Tg (2.5 µM)-induced Ca^{2+} fluxes measured as in A. (**D**) Defective Tg-induced Ca^{2+} fluxes demonstrated using cyclopiazonic acid (CPA; 1 µM). (**E–F**) Tg (2.5 µM)-induced Ca^{2+} fluxes measured by confocal

Figure 8 continued on next page

Figure 8 continued

imaging of stably expressed genetic cytoplasmic Ca^{2+} sensors: cytoplasmic sensor GCaMP6s (**E**) and plasma membrane-localized sensor GCaMP6s-CAAX (**F**). (**G**) Tg (2.5 μM)-induced Ca^{2+} fluxes in Fluo4 AM-loaded control MDA-MB-468 (EHD2-negative) vs its CRISPRa derivative (EHD2-expressing). (**H–I**) Tg (2.5 μM)-induced Ca^{2+} fluxes in Fluo4 AM-loaded control and *CAV1*-KO TNBC lines. Mean +/- SEM of peak fluorescence intensity (n=3, *p<0.05) is shown below all panels.

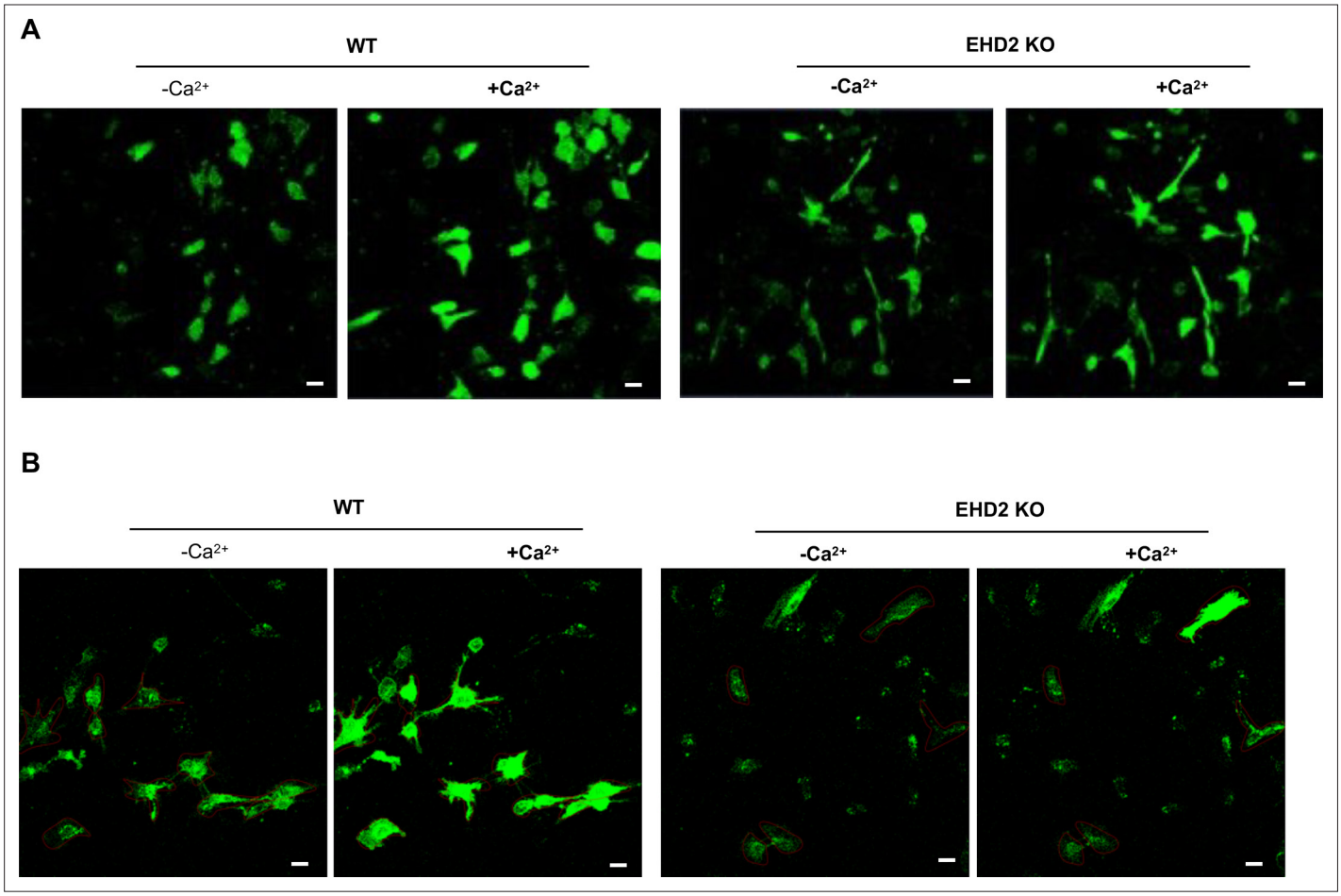

Figure 8—figure supplement 1. Loss of EHD2 decreased SOCE in TNBC cells. Enhancement of reporter fluorescence measured upon thapsigargin (2.5 μM) and Ca^{2+} (2 mM), immunofluorescent images of SOCE before and after Ca^{2+} addition from Control and *EHD2*-KO Hs578T cells engineered with the cytoplasmic calcium sensor GCaMP6s (**A**) or plasma membrane-localized calcium sensor GCaMP6s-CAAX (**B**). Scale bar, 10 μm.

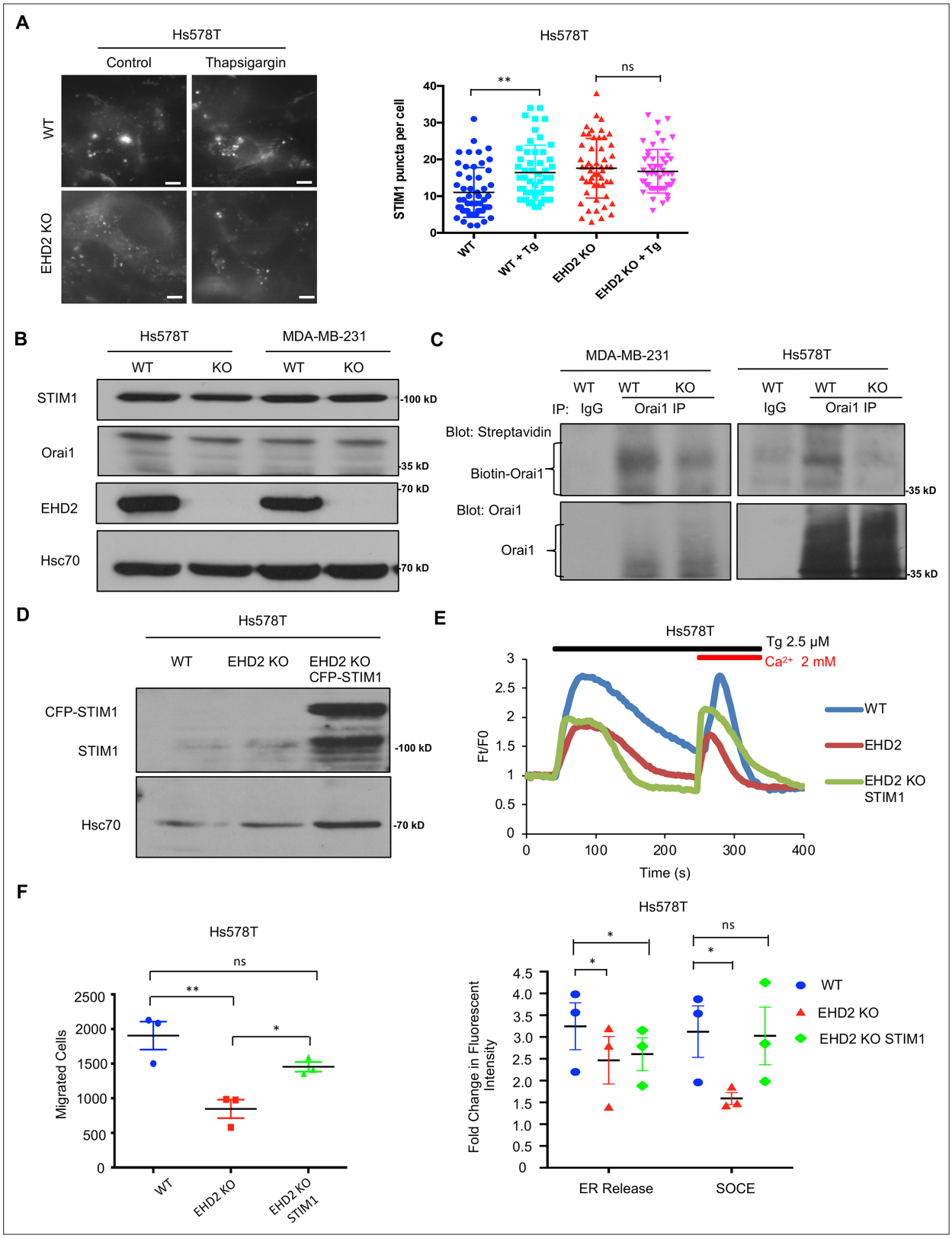

Figure 9. EHD2 regulates SOCE through STIM1-Orai1. (**A**) CFP-STIM1-trasnfected cells were analyzed for plasma membrane proximal fluorescent puncta by TIRF microscopy, without (control) or with thapsigargin treatment (2.5 µM, 5 min). Left, representative TIRF images; Right, Mean +/- SEM of STIM1 puncta/cell, ** p<0.01. Scale bar, 5 µm. (**B**) Immunoblotting to show comparable total STIM1 and Orai1 levels in control vs *EHD2*-KO TNBC lines; Hsc70, loading control. (**C**) Reduced cell surface levels of Orai1 in *EHD2*-KO cells. Live cell surface biotinylated cell Orai-1 immunoprecipitates blotted

Figure 9 continued on next page

Figure 9 continued

with Streptavidin (top) and Orai1 (bottom). (**D**) Anti-STIM1 immunoblotting to show stable overexpression of STIM1-CFP in *EHD2*-KO Hs578T cells. (**E**) Partial rescue of SOCE by ectopic CFP-STIM1 overexpression analyzed upon thapsigargin (Tg; 2.5 μM) treatment of Fluo 4 AM-loaded cells. Bottom, Mean +/- SEM of peak fluorescence, N=3; *p<0.05. (**F**) Partial rescue of Transwell cell migration defect by CFP-STIM1 overexpression in *EHD2*-KO cells. Mean +/- SEM of migrated cells (input 10 K); n=3; *p<0.05.

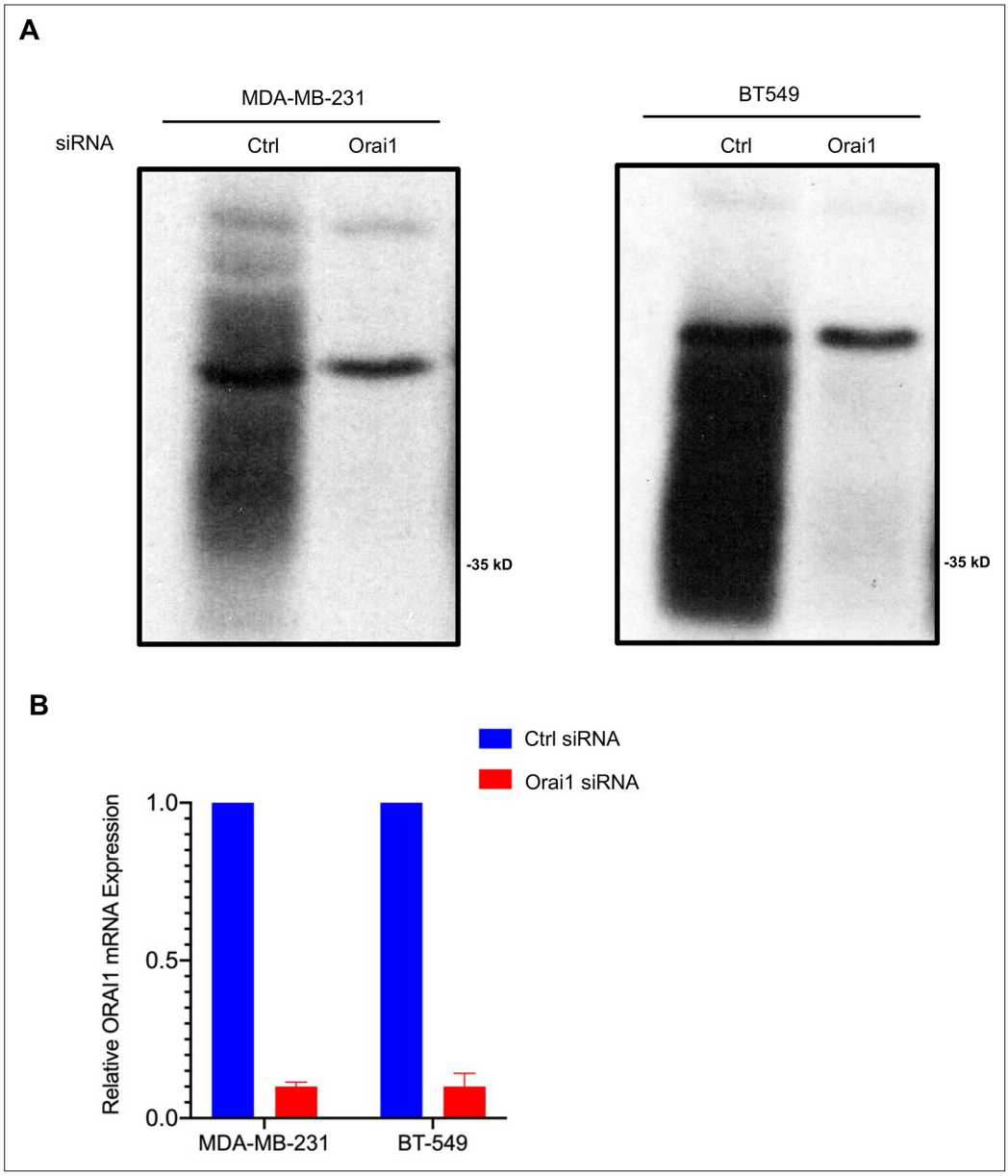

Figure 9—figure supplement 1. Validation of ORAI1 antibody in triple negative breast cancer cell lines. MDA-MB-231 and BT549 were transfected with either control siRNA or *Orai1* siRNA for 72 h. (**A**) Whole cell lysates were subjected to immunoblotting with anti-Orai1 (cat. # O8264, Sigma). Orai1appears as a smear. (**B**) Total RNA was used for *Orai1* qPCR to establish successful and specific knockdown of *Orai1* mRNA expression in *Orai1* siRNA transfected cells.

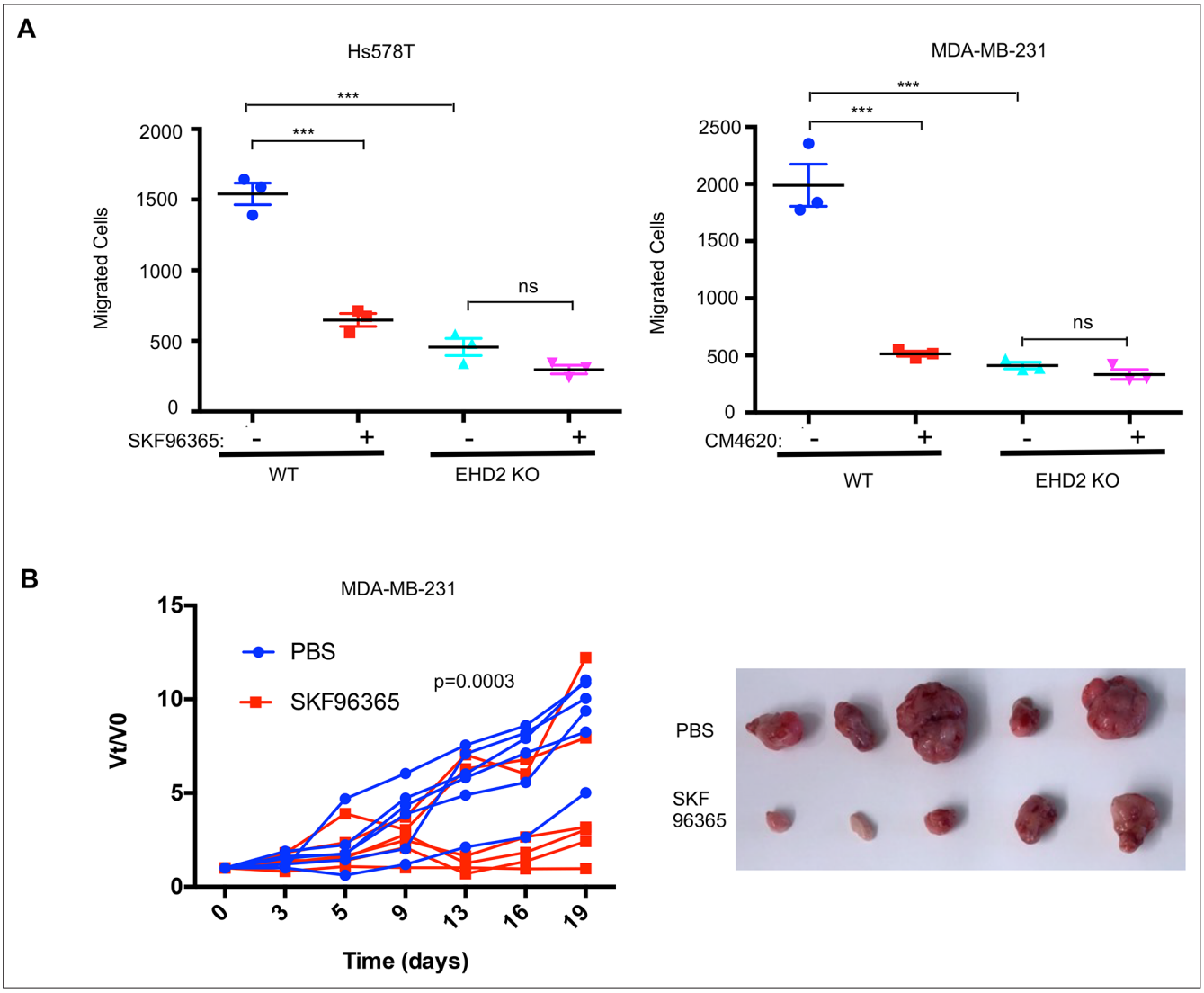

Figure 10. EHD2 expression determines the relative functional impact of SOCE inhibition in TNBC cells. (**A**) Impact of SOCE inhibitors SKF96365 (10 μM) or CM4620 (10 μM) Transwell migration of Control vs *EHD2*-KO TNBC cell lines. Mean +/- SEM of n=3; ***p<0.001. (**B**) SOCE inhibition reduces TNBC tumorigenesis. Nude mice (8/group) bearing orthotopic MDA-MB-231 ($3x10^6$) cell tumors (average 4–5 mm in diameter) were administered 10 mg/kg SKF96365 (in PBS) or PBS intraperitoneally and change in tumor volumes (V_t/V_0) monitored over time and differences analyzed by two-way ANOVA. Right, representative tumor images.